The influence of substituted indigo derivatives on the preparation and properties of "Maya" pigments

Michael Gerlach [a,b,1], Justus Koedel [c,d,1], Sebastian Seibt [b,d], Benjamin Baumgärtner [b],
Christoph Callsen [e], Gundula Voss [f], Florian Puchtler [g], Andy Weidinger [c], Georg Puchas [h],
Daniel Leykam [i], Volker Altstaedt [e], Rainer Schobert [d], Holger Ruckdäschel [e,**],
Bernhard Biersack [d,*]

[a] Physikalische Technik/Informatik, Westsächsische Hochschule Zwickau, Kornmarkt 1, 08056 Zwickau, Germany
[b] Linseis Messgeräte GmbH, Vielitzerstrasse 43, 95100 Selb, Germany
[c] Fachgruppe Chemie, Wirtschaftswissenschaftliches und Naturwissenschaftlich-Technologisches Gymnasium Bayreuth, Am Sportpark 1, 95448 Bayreuth, Germany
[d] Organic Chemistry I, University of Bayreuth, Universitätsstraße 30, 95447 Bayreuth, Germany
[e] Department of Polymer Engineering, University of Bayreuth, Universitätsstraße 30, 95447 Bayreuth, Germany
[f] Bioorganic Chemistry, University of Bayreuth, Universitätsstraße 30, 95447 Bayreuth, Germany
[g] Inorganic Chemistry I, University of Bayreuth, Universitätsstraße 30, 95447 Bayreuth, Germany
[h] Ceramic Materials Engineering, University of Bayreuth, Prof.-Rüdiger-Bormann-Str. 1, 95447, Bayreuth, Germany
[i] Electrochemical Process Engineering, University of Bayreuth, Universitätsstraße 30, 95447 Bayreuth, Germany

ARTICLE INFO

ABSTRACT

A small series of indigo derivatives were mixed with palygorskite or sepiolite, respectively, and heated at 150 °C overnight in order to prepare stable pigments. While mixtures with violet halo-indigos such as Tyrian Purple (6,6′-dibromoindigo) and its difluoro- and dichloro-derivatives formed blue pigments with a slight greenish hue upon heating, alkoxy-indigo derivatives turned olive green during the heating process when mixed with palygorskite or sepiolite. Mixtures of isatin and indigo with palygorsite led to the formation of green pigments. The pigments were analyzed by spectroscopy (UV-VIS and Raman) and electron microscopy. Thermal studies were carried out and the obtained pigments were stable at temperatures of up to 250 °C. Maya Blue and pigment samples derived from 6,6′-dichloroindigo were tested for their flame retarding properties in mixtures with cellulose acetate and both additives led to distinct heat release rate reductions.

1. Introduction

The identification of robust ancient blue silicate pigments such as Egyptian Blue ($CaCuSi_4O_{10}$), Han Blue ($BaCuSi_4O_{10}$), Ultramarine Blue ($(Na,Ca)_8(AlSiO_{12})$), and Maya Blue ($x \cdot$ indigo $\cdot$ $(Mg,Al)_4Si_8(O,OH, H_2O)_{24}$) indicates the amazing knowledge and skills of dyers in ancient times [1,2]. Maya Blue was used as a pigment by the people of the Maya culture in Mesoamerica (modern Mexico, Guatemala, Nicaragua and Belize) since the 1st millennium AD and it was first described by Merwin (1931) before Gettens and Stout dubbed the pigment "Maya Blue" (1942) [3]. Maya Blue has an inorganic structure based on colorless palygorskite clay (a.k.a. attapulgite) with indigo as colorizing agent, and

the synthesis of Maya Blue by mixing palygorskite with a small amount of indigo, followed by heating for several hours/days was first described by van Olphen in 1966 [3,4]. The indigo molecules interact with the palygorskite or the related sepiolite clay upon heating and are incorporated into the channels of the clay host structure whereupon the color of the indigo molecules changes from blue to turquoise or greenish light blue [5,6]. Spectroscopic and electrochemical data indicated an interaction of the indigo molecules with the palygorskite or sepiolite clay to form dehydroindigo molecules upon tautomerization to indigo hemienol followed by oxidation, which led to the characteristic greenish blue color of Maya Blue [7–10]. The stability of the Maya Blue pigment is outstanding and includes exposure to concentrated acids. Only

treatment with hot acids led to decomposition of the pigment [11].

Similarly, the ancient ochre pigment Maya Yellow was identified as the composition of palygorskite with the orange dye isatin (1*H*-indole-2,3-dione) [12,13]. Further new pigments based on palygorskite and synthetic dyes such as thioindigo ("Maya Pink"), CR-X-GRL ("Maya Red"), or methyl violet ("Maya Violet"), various anthraquinone dyes and other aromatic dyes were disclosed [14–17].

The blue organic dye indigo has played a significant economic role for thousands of years and natural indigo was obtained from plants such as *Indigofera tinctoria* in India and *Isatis tinctoria* (woad) in Europe [18, 19]. Synthetic indigo has largely replaced natural indigo since Adolph von Baeyer described his synthesis of indigo [20]. The violet derivative 6,6′-dibromoindigo was identified as the colorizing agent of Tyrian purple (Royal purple), which is produced by the sea snail *Murex brandaris* and other mollusks [21]. Synthetic 6,6′-dibromoindigo can be prepared analogously to indigo but the synthesis of the 4-bromo-2-nitrobenzaldehyde precursor became a crucial step [21,22]. Meanwhile, more convenient routes to Tyrian purple were disclosed starting from halo-indoles and the preparation of the fluoro-, chloro- and iodo-analogs of 6,6′-dibromoindigo was also published [22–25]. In addition, green indigo derivatives with alkoxy substituents were described [25,26].

Aside their application as dyes, both indigo and 6,6′-dibromoindigo were investigated as modern natural organic semiconductors [27,28]. Hence, the knowledge of the interaction of indigos with other materials is of significance. Violet halo- and dark green alkoxy indigo derivatives have not been investigated in mixtures with palygorskite or sepiolite, yet. Two works only observed that the Maya Blue analog of 6,6′-dibromoindigo is blue but no detailed analyses were published [21,29].

In this study, the processes of pigment formation of palygorskite or sepiolite mixed with various halo- or alkoxyindigo derivatives were investigated and compared with genuine Maya Blue samples. In addition, Maya Blue and analogous samples derived from 6,6′-dichloroindigo were tested as flame retardants in mixtures with the re-growing bioplastic cellulose acetate. Pigments can be applied topically as paints or lacquers, or can be directly mixed with various flammable materials. However, several clay materials including layered silicates have shown considerable flame retarding effects which warrants the investigation of Maya pigments as possible flame retardants [30].

2. Experimental section

2.1. Materials

Cellulose acetate (average $M_n \sim 30.000$ g/mol) was purchased from Sigma-Aldrich. Palygorskite (attapulgite), sepiolite, synthetic indigo, thioindigo, and isatin were purchased from Aldrich. The synthesis of the indigo derivatives 6,6′-difluoroindigo, 6,6′-dichloroindigo, 6,6′-dibromoindigo, 5,5′,6,6′-tetramethoxyindigo, and 5,5′,6,6′-dimethylenedioxyindigo (Fig. 1) was described before [22–25]. Maya Blue (two variants prepared from the palygorskite mixture with 1 % or 2 % indigo), its sepiolite analog (Sepi Blue) and the corresponding analogs with thioindigo (Maya Thio) were prepared from indigo or thioindigo, respectively, and palygorskite or sepiolite according to literature procedures [4,14].

2.2. Preparation of the new pigments

2.2.1. Maya-Cl2 1 %

6,6′-Dichloroindigo (100 mg) and palygorskite (9.9 g) were thoroughly mixed in a mortar and the obtained violet mixture was heated at 150 °C for 22 h. The violet mixture turned blue during this heating process. The resulting blue powder was washed with hot acetone (2 × 7 h) via Soxhlet extraction. The remaining powder was dried in vacuum. Yield: 9.2 g; blue solid.
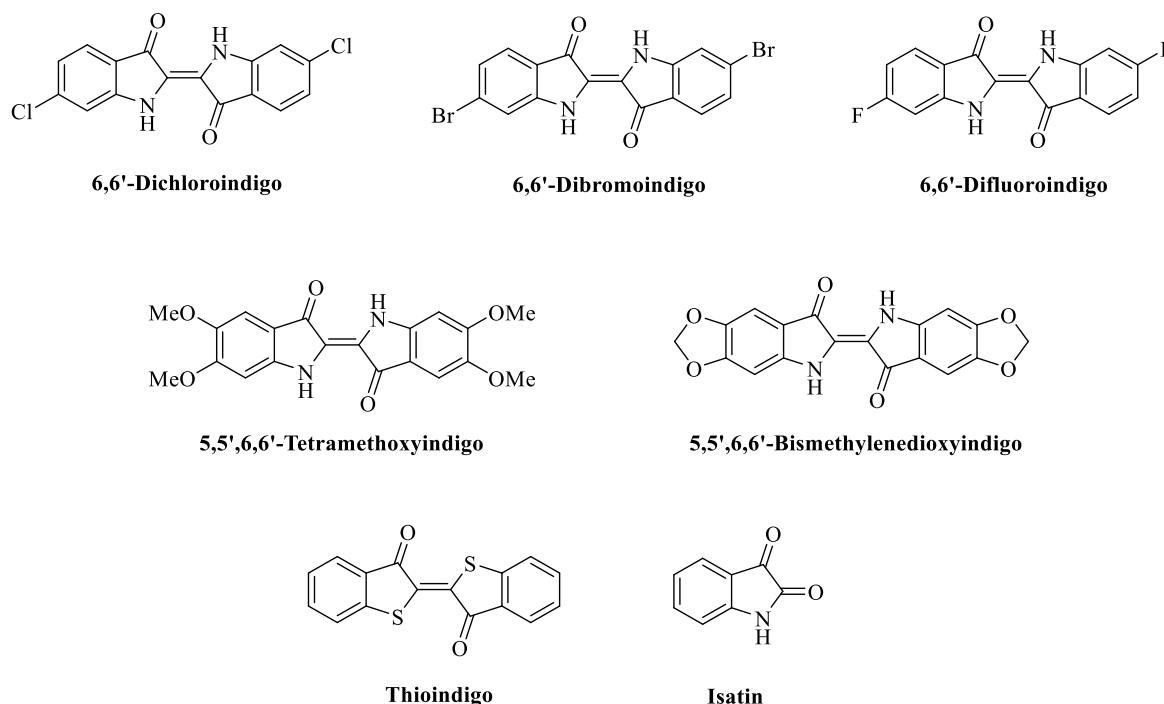
2.2.2. Maya-Cl2 2 %

6,6′-Dichloroindigo (200 mg) and palygorskite (9.8 g) were thoroughly mixed in a mortar and the obtained violet mixture was heated at 150 °C for 22 h. The violet mixture turned blue during this heating process. The resulting blue powder was washed with hot acetone (2 × 7 h) via Soxhlet extraction. The remaining powder was dried in vacuum. Yield: 9.2 g; blue solid.

6,6'-Dichloroindigo **6,6'-Dibromoindigo** **6,6'-Difluoroindigo**

5,5',6,6'-Tetramethoxyindigo **5,5',6,6'-Bismethylenedioxyindigo**

Thioindigo **Isatin**

Fig. 1. Indigo derivatives used in this study for the preparation of pigments.

2.2.3. Maya-Br2 1 %

Analogously to the synthesis of Maya-Cl2, Maya-Br2 was obtained from 6,6′-dibromoindigo (100 mg) and palygorskite (9.9 g) after washing with with hot acetone (2 × 7 h) via Soxhlet extraction. Yield: 9.2 g; light-blue solid.

2.2.4. Maya-F2 1 %

Analogously to the synthesis of Maya-Cl2, Maya-F2 was obtained from 6,6′-difluoroindigo (100 mg) and palygorskite (9.9 g) after washing with hot acetone (2 × 7 h) via Soxhlet extraction. Yield: 9.2 g; light-blue solid.

2.2.5. Maya-MeO4 1 %

Analogously to the synthesis of Maya-Cl2, Maya-MeO4 (1 %) was obtained from 5,5′,6,6′-tetramethoxyindigo (100 mg) and palygorskite (9.9 g) after washing with hot acetone (2 × 7 h) via Soxhlet extraction. Yield: 9.2 g; green solid.

2.2.6. Maya-OMeO2 1 %

Analogously to the synthesis of Maya-Cl2, Maya-OMeO2 (1 %) was obtained from 5,5′,6,6′-bismethylenedioxyindigo (100 mg) and palygorskite (9.9 g) after washing with hot acetone (2 × 7 h) via Soxhlet extraction. Yield: 9.2 g; green solid.

2.2.7. Maya Yellow 2 %

Analogously to the synthesis of Maya-Cl2, Maya-Yellow (2 %) was obtained from isatin (200 mg) and palygorskite (9.8 g) after washing with hot acetone (2 × 7 h) via Soxhlet extraction. Yield: 9.1 g; off-white solid.

2.2.8. Maya Green 15

Isatin (500 mg), indigo (100 mg) and palygorskite (9.4 g) were thoroughly mixed in a mortar and the obtained blue mixture was heated at 150 °C for 22 h. The blue color of the powder turned green during the heating process. The obtained powder was washed with hot acetone (2 × 7 h) via Soxhlet extraction. The product powder was dried in vacuum. Yield: 9.8 g; green solid.

2.2.9. Maya Green 25

Analogously to the synthesis of Maya Green 15, Maya Green 25 was obtained from isatin (500 mg), indigo (200 mg) and palygorskite (9.3 g) after washing with hot acetone (2 × 7 h) via Soxhlet extraction. Yield: 9.8 g; bluegreen solid.

2.2.10. Sepi-Cl2 1 %

6,6′-Dichloroindigo (50 mg) and sepiolite (4.95 g) were thoroughly mixed in a mortar and the obtained violet mixture was heated at 150 °C for 22 h. The violet mixture turned blue during this heating process. The obtained powder was washed with hot acetone (2 × 7 h) via Soxhlet extraction. The powder was dried in vacuum. Yield: 4.3 g; blue solid.

2.2.11. Sepi-Br2 1 %

Analogously to the synthesis of Sepi-Cl2, Sepi-Br2 was obtained from 6,6′-dibromoindigo (50 mg) and sepiolite (4.95 g) after washing with hot acetone (2 × 7 h) via Soxhlet extraction. Yield: 4.4 g; blue solid. The preparation of a blue pigment from sepiolite and a higher amount of 6,6′-dibromoindigo (32 mg 6,6′-dibromoindigo per gram sepiolite) as starting material was published recently [29].

2.3. XRD spectroscopy

Qualitative X-Ray diffraction measurements were performed on a Bruker D8 Advance (Bruker, USA) in order to analyze the phase composition of the different pigments. The investigation was carried out in the range between $10° < 2θ < 90°$, with a step size of $0.02°$ and a measuring time of 0.5 s per step.

2.4. Solid state UV-VIS spectroscopy

Solid-state UV-VIS spectra of pigment samples were measured on an AvaSpec 2048 (Avantes, Apeldoorn, the Netherlands) supplied with an AvaLight-DH-SBAL light source at room temperature.

2.5. Thermal gravimetric analysis and differential scanning calorimetry

Thermal gravimetric analysis (TGA) and differential scanning calorimetry (DSC) of the pigments were performed on a Linseis STA PT1600 analyzer from Linseis (Selb, Germany) according to ISO 11358–1:2014. The sensor head used was a platinum type S system with Al_2O_3 crucibles of 0.25 mL volume. All measurements were performed with 20 mg of the test sample at a constant heating rate of 10 K/min in air (flow rate 6 L/h) up to 1000 °C. Enthalpy was calibrated with standard reference measurements (In/Pb/Zn/Au).

A newly designed Chip-DSC device was applied for video-documented DSC measurements (Fig. 2). The advantage of this Chip-DSC is the possibility to adapt a camera to the measurement cell in order to determine melting behavior and color changes of the samples in real time. The samples where measured in 40 µL Al-crucibles. Initially, the samples where heated up to 250 °C with a heating rate of 50 K/min. In the second step the maximum temperature was set to 400 °C and the heating rate was lowered to 35 K/min to get a higher temperature dependent resolution. In order to receive more reliable results for the neighboring transitions in the lower temperature range, the heating rate was corrected to 20 K/min. Isothermal experiments were carried out at 225 °C. Pictures of the samples were recorded every 5 s. Isothermal temperature stability experiments were carried out at 230 °C, 250 °C and 270 °C (each for 15 min), respectively.

To determine the color values for RGB, as well as for CIE LAB and CIE XYZ, the images from Tables 1 and 2 were used. By using a free software (Color Picker V7.8.3), circular sections of the images were selected in
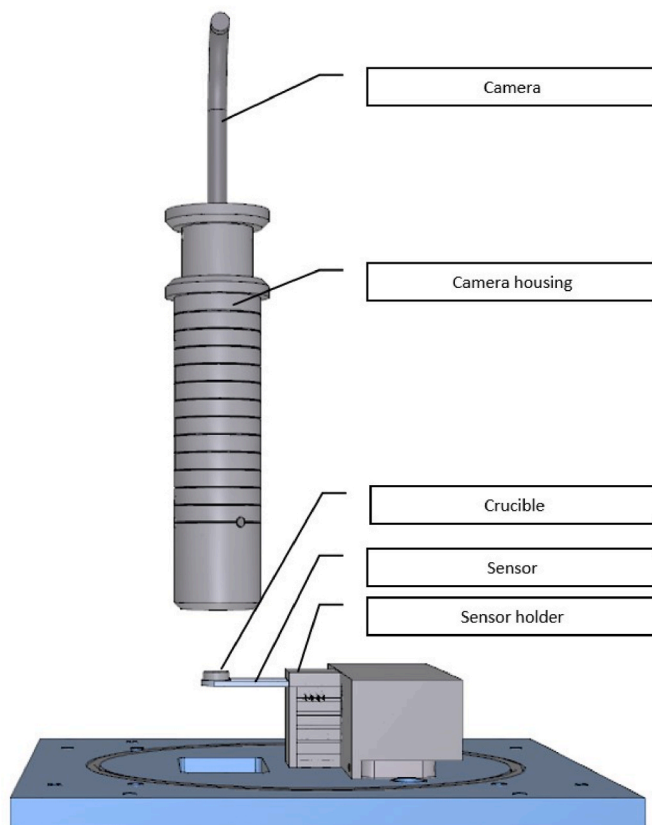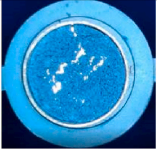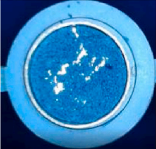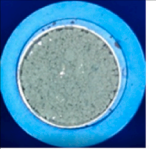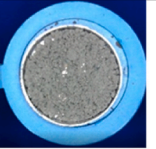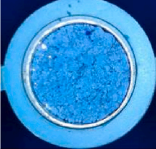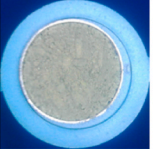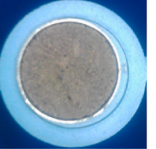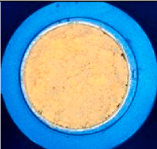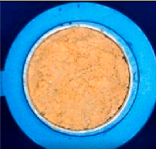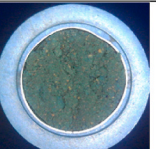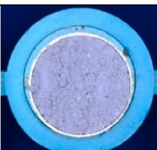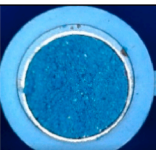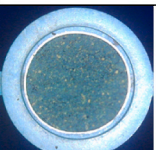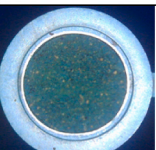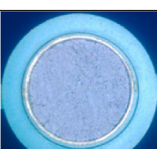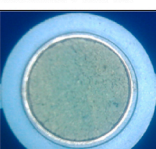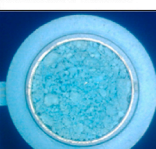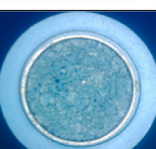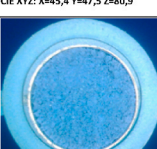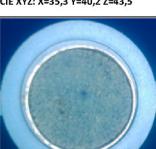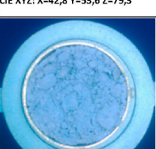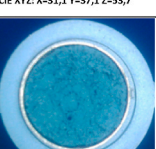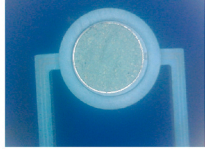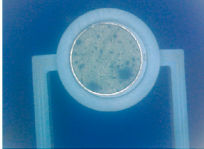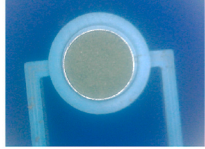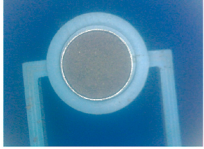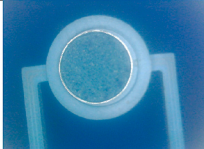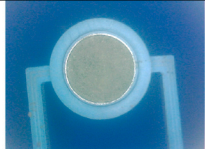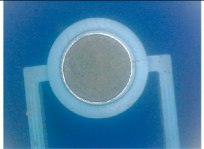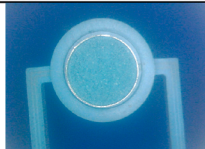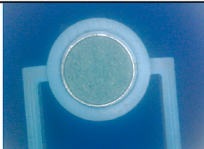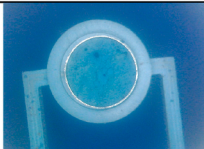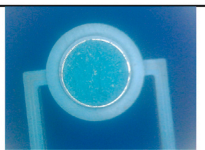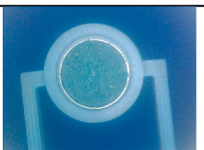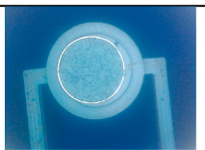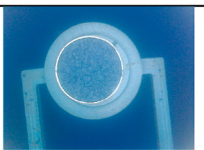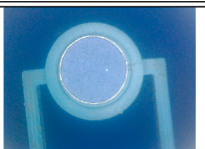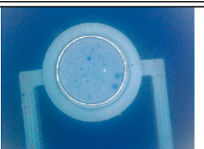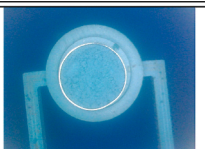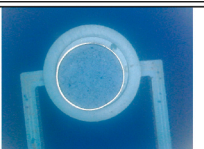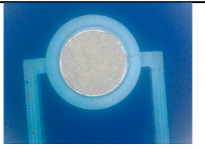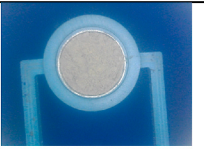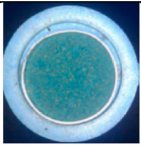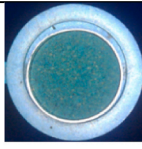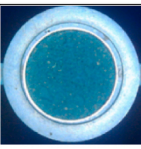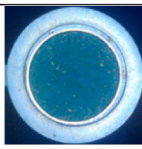

Fig. 2. Chip-DSC 10 device with attached video camera.

Table 1

Colors of mixtures before and after heating to 250 °C. Palygorskite and sepiolite are shown as untreated reference compounds.

Sample	Mixture at r. t.	Mixture upon heating to 250 °C	Sample	Mixture at r. t.	Mixture upon heating to 250 °C
Maya Blue (1%)	R:60 G:162 B:220 CIE LAB: L=63,6 A=-10,9 B=-37,4 CIE XYZ: X=27,9 Y=32,3 Z=72,5	R:43 G:150 B:203 CIE LAB: L=58,7 A=-11,5 B=-35,6 CIE XYZ: X=22,7 Y=26,7 Z=60,4	Maya MeO4 (1%)	RGB: R:147 G:172 B:164 CIE LAB: L=68,3 A=-10,2 B=1,2 CIE XYZ: X=33,5 Y=38,4 Z=40,8	RGB: R:141 G:143 B:140 CIE LAB: L=59,2 A=-1,3 B=1,3 CIE XYZ: X=25,5 Y=27,2 Z=28,7
Maya Thio (1%)	R:196 G:185 B:224 CIE LAB: L=76,8 A=11,6 B=-18,6 CIE XYZ: X=53,1 Y=51,3 Z=77,6	R:78 G:163 B:237 CIE LAB: L=64,9 A=-2,6 B=-44,7 CIE XYZ: X=31,5 Y=33,9 Z=85,0	Maya OMeO2 (1%)	RGB: R:171 G:178 B:171 CIE LAB: L=71,9 A-3,8 B=2,7 CIE XYZ: X=40,1 Y=43,4 Z=44,8	RGB: R:144 G:142 B:138 CIE LAB: L=59,1 A=-0,0 B=2,4 CIE XYZ: X=25,8 Y=27,5 Z=28,4
Maya Yellow (2%)	R:246 G:202 B:134 CIE LAB: L=83,6 A=6,7 B=39,6 CIE XYZ: X=63,1 Y=63,4 Z=31,5	RGB: R:237 G:172 B:108 CIE LAB: L=75,1 A=16,4 B=42,4 CIE XYZ: X=52,0 Y=48,4 Z=20,5	Maya Green 15	RGB: R:115 G:150 B:144 CIE LAB: L=59,4 A=-13,4 B=-0,8 CIE XYZ: X=23,0 Y=27,5 Z=30,5	RGB: R:92 G:119 B:108 CIE LAB: L=47,7 A=-12,3 B=2,8 CIE XYZ: X=13,7 Y=16,6 Z=16,6
Maya Cl2 (1%)	RGB: R:165 G:172 B:221 CIE LAB: L=71,4 A=8,2 B=-25,5 CIE XYZ: X=43,3 Y=42,7 Z=74,4	RGB: R:35 G:142 B:190 CIE LAB: L=55,5 A=-12,5 B=-33,2 CIE XYZ: X=19,7 Y=23,4 Z=52,2	Maya Green 25	RGB: R:94 G:137 B:145 CIE LAB: L=53,9 A=-12,6 B=-9,0 CIE XYZ: X=18,3 Y=21,9 Z=30,1	RGB: R:67 G:111 B:115 CIE LAB: L=43,9 A=-14,0 B=-7,0 CIE XYZ: X=11,1 Y=13,8 Z=18,3
Maya-Br2 (1%)	RGB: R:157 G:185 B:229 CIE LAB: L=74,5 A=0,7 B=-25,1 CIE XYZ: X=45,4 Y=47,5 Z=80,9	RGB: R:139 G:178 B:169 CIE LAB: L=69,6 A=-15,0 B=0,3 CIE XYZ: X=35,3 Y=40,2 Z=43,5	Sepi Blue (1%)	RGB: R:114 G:207 B:225 CIE LAB: L=78,3 A=-22,9 B=-17,5 CIE XYZ: X=42,8 Y=53,6 Z=79,3	RGB: R:114 G:173 B:189 CIE LAB: L=67,4 A=-15,0 B=-14,2 CIE XYZ: X=31,1 Y=37,1 Z=53,7
Maya-F2 (1%)	RGB: R:89 G:178 B:230 CIE LAB: L=69,6 A=-9,7 B=-33,5 CIE XYZ: X=35,2 Y=40,2 Z=80,8	RGB: R:115 G:163 B:171 CIE LAB: L=63,9 A=-14,0 B=-9,3 CIE XYZ: X=27,5 Y=32,8 Z=43,4	Sepi-Cl2 (1%)	RGB: R:121 G:185 B:232 CIE LAB: L=72,6 A=-7,9 B=-29,8 CIE XYZ: X=39,8 Y=44,6 Z=82,9	RGB: R:70 G:160 B:183 CIE LAB: L=61,5 A=-19,7 B=-19,9 CIE XYZ: X=23,6 Y=29,9 Z=49,3
Palygorskite (pure)	RGB: R:209 G:213 B:209 CIE LAB: L=84,9 A=-2,1 B=1,5 CIE XYZ: X=61,6 Y=65,7 Z=69,8	RGB: R:208 G:212 B:207 CIE LAB: L=84,5 A=-2,3 B=2,0 CIE XYZ: X=60,8 Y=65,0 Z=68,4	Sepiolite (pure)	RGB: R:243 G:244 B:232 CIE LAB: L=95,8 A=-2,4 B=5,6 CIE XYZ: X=83,9 Y=89,6 Z=89,2	RGB: R:224 G:224 B:219 CIE LAB: L=89,1 A=-0,9 B=2,4 CIE XYZ: X=70,8 Y=74,3 Z=77,7

Table 2
Colors and temperature stability of pure pigments.

Sample	Room temperature	230-270°C	Sample	Room temperature	230-270°C
Maya Blue (1%)	RGB: R:144 G:191 B:193 CIE LAB: L=74,2 A=−14,9 B=−6,1 CIE XYZ: X=39,8 Y=47,0 Z=57,4	RGB: R:130 G:170 B:176 CIE LAB: L=67,0 A=−12,0 B=−7,5 CIE XYZ: X=31,4 Y=36,6 Z=46,5	**Maya MeO4 (1%)**	RGB: R:138 G:162 B:153 CIE LAB: L=64,6 A=−10,2 B=1,9 CIE XYZ: X=29,2 Y=33,5 Z=35,1	RGB: R:130 G:148 B:152 CIE LAB: L=60,1 A=−5,5 B=−4,3 CIE XYZ: X=25,5 Y=28,2 Z=33,8
Maya F2 (1%)	RGB: R:80 G:181 B:205 CIE LAB: L=68,9 A=−22,2 B=−20,9 CIE XYZ: X=30,2 Y=39,2 Z=63,7	RGB: R:91 G:159 B:180 CIE LAB: L=61,9 A=−15,7 B=−17,6 CIE XYZ: X=25,0 Y=30,3 Z=47,7	**Maya OMeO2 (1%)**	RGB: R:150 G:171 B:160 CIE LAB: L=68,1 A=−9,5 B=3,2 CIE XYZ: X=33,5 Y=38,1 Z=38,9	RGB: R:129 G:148 B:147 CIE LAB: L=59,8 A=−7,0 B=−1,8 CIE XYZ: X=24,9 Y=28,0 Z=31,7
Maya Br2 (1%)	RGB: R:111 G:190 B:203 CIE LAB: L=72,6 A=−20,9 B=−14,1 CIE XYZ: X=35,7 Y=44,5 Z=63,2	RGB: R:118 G:170 B:173 CIE LAB: L=66,2 A=−16,3 B=−7,1 CIE XYZ: X=29,4 Y=35,6 Z=44,9	**Sepi Blue (1%)**	RGB: R:71 G:190 B:219 CIE LAB: L=71,7 A=−24,0 B=−24,2 CIE XYZ: X=33,8 Y=43,3 Z=73,6	RGB: R:77 G:165 B:193 CIE LAB: L=63,6 A=−18,0 B=−22,3 CIE XYZ: X=26,1 Y=32,3 Z=55,3
Maya Cl2 (1%)	RGB: R:85 G:187 B:202 CIE LAB: L=70,7 A=−25,2 B=−16,5 CIE XYZ: X=32,2 Y=41,7 Z=62,2	RGB: R:91 G:164 B:176 CIE LAB: L=63,3 A=−19,5 B=−13,3 CIE XYZ: X=25,4 Y=31,9 Z=45,9	**Sepi Cl2 (1%)**	RGB: R:117 G:192 B:207 CIE LAB: L=73,5 A=−19,4 B=−14,8 CIE XYZ: X=37,4 Y=46,0 Z=65,9	RGB: R:91 G:157 B:191 CIE LAB: L=61,7 A=−11,4 B=−24,0 CIE XYZ: X=25,8 Y=30,1 Z=53,7
Maya Thio (1%)	RGB: R:142 G:182 B:226 CIE LAB: L=72,7 A=−2,6 B=−26,3 CIE XYZ: X=41,6 Y=44,7 Z=78,4	RGB: R:124 G:178 B:208 CIE LAB: L=70,0 A=−10,0 B=−20,8 CIE XYZ: X=35,6 Y=40,7 Z=65,6	**Sepi Br2 (1%)**	RGB: R:110 G:191 B:214 CIE LAB: L=73,2 A=−18,6 B=−19,2 CIE XYZ: X=37,2 Y=45,4 Z=70,4	RGB: R:99 G:164 B:197 CIE LAB: L=64,3 A=−11,7 B=−23,3 CIE XYZ: X=28,5 Y=33,2 Z=58,3
Maya Yellow (2%)	RGB: R:193 G:193 B:186 CIE LAB: L=77,9 A=−1,2 B=3,5 CIE XYZ: X=49,9 Y=53,0 Z=54,1	RGB: R:181 G:182 B:178 CIE LAB: L=73,9 A=−1,0 B=1,9 CIE XYZ: X=43,8 Y=46,5 Z=48,8	**Maya Green 15**	RGB: R:80 G:152 B:152 CIE LAB: L=58,4 A=−22,5 B=−7,0 CIE XYZ: X=20,2 Y=26,4 Z=33,7	RGB: R:75 G:138 B:140 CIE LAB: L=53,6 A=−19,7 B=−7,3 CIE XYZ: X=16,7 Y=21,6 Z=28,1
			Maya Green 25	RGB: R:50 G:138 B:157 CIE LAB: L=53,3 A=−19,5 B=−17,7 CIE XYZ: X=16,5 Y=21,3 Z=35,1	RGB: R:47 G:122 B:146 CIE LAB: L=47,8 A=−15,1 B=−19,8 CIE XYZ: X=13,3 Y=16,6 Z=29,7

such a way that the largest possible area covered with sample material was evaluated. A corresponding mean value was determined without distorting the result by coloring of the background or the aluminum crucible.

2.6. Raman spectroscopy

The pigment was poured into an aluminum sample crucible used for the chip DSC and then smoothed out. The sample was placed in the Chip DSC and the sample chamber was equipped with a customized Raman sensor holder. The Raman shift of the different samples was measured with a Raman spectrometer from Wasatch Photonics (Morrisville, USA) and analyzed with the ENLIGHTEN 3.7.5. software. In the first step, the dark spectrum without the LASER source switched on is analyzed with an averaging of 5. This is subtracted from all measurements to reduce noise. The laser has a nominal wavelength of 785 nm and the measurement is carried out in the range from 267 to 2005 cm^{-1}. The LASER power for the reference samples of sepiolite and palygorskite was 450 mW and for all samples with pigments 250 mW. The integration time of the detector was 1200 ms and 2000 ms, respectively. To reduce noise, the scan was repeated 300 times and averaged. In the post scan processing, the signal was averaged with a boxcar smoothing filter with a half-width of the Heavyside-function of 2 pixels, which corresponds to an averaging of 5 pixels. The fluorescence background was deduced with an aptive iteratively reweighted penalized least squares (airPLS) algorithm. The system response was normalized with the function 'Raman Intensity Correction' against a SRM NIST standard, which leads to an improvement of the generated Raman spectrum.

2.7. Scanning electron microscopy

Small fragments of the sample were mounted on a standard sample holder by conductive adhesion graphite-pad (Plano, Germany) and sputtered with platinum using a Cressington HR208 sputter coater (Cressington, UK). Scanning electron microscopy was performed on a Zeiss Ultra plus (Zeiss, Germany) operating at 3 kV with an Everhart-Thornley detector for secondary electron detection.

2.8. Combustion analyses

Mixtures of cellulose acetate (medium M_n ~ 30.000 g/mol, Sigma-Aldrich) and Maya Blue or Maya-Cl2 (4.4 %, w/w) were homogenized in a ball mill (Retsch PM 100) with 250 rpm for 1 h. The samples were pressed at 210 °C and 50 kN for 5 min in order to prepare plates of 100 x 100 × 3 mm^3 for the cone calorimetric analysis. Cone calorimeter experiments with the cellulose acetate plates were performed with an iCone Plus Calorimeter from Fire Testing Technology, UK (35 kW/m^2 heat flux with horizontal orientation of the samples, 25 mm distance) according to ASTM E 1354.

3. Results and discussion

3.1. Pigment synthesis and analysis

The pure pigments were prepared analogously to a literature procedure by heating at 150 °C for 22 h followed by repeated washing with hot acetone [4,14]. The pigments were dubbed "Maya" when based on palygorskite while the "Sepi" pigments derived from sepiolite. Changes in the color were observed for most mixtures. The violet dyes 6, 6′-difluoro- (F2), 6,6′-dichloro- (Cl2), and 6,6′-dibromoindigo (Br2) turned blue upon heating when admixed with palygorskite or sepiolite. Such an effect was also described for solutions of 6,6′-dibromoindigo and was explained by the absence of interactions between the halo-indigo molecules in solution, and upon intercalation into the clay in our case leading to the formation of halogenated dehydroindigo derivatives in the clay [21]. In addition, the formation of halogenated dehydroindigo

derivatives in the clay in analogy to the synthesis of blue-green Maya Blue from deep blue indigo can play a role in this remarkable color shift [8–10]. Differences in the colors between palygorskite and sepiolite pigments made from the same indigo derivative (e.g., Maya-Cl2 and Sepi-Cl2) can be explained by characteristic properties of the used clay materials. Palygorskite and sepiolite share fibrous morphologies but display different surface properties [31]. For instance, it was shown that palygorskite has lower surface energy, larger specific interactions, and higher nanomorphology indices than sepiolite [32]. The deep green dyes 5,5′,6,6′-tetramethoxyindigo (MeO4) and 5,5′,6,6′-bismethylenedioxyindigo (OMeO2) turned into olive green in heated mixtures with palygorskite. The color changes of various mixed starting materials upon heating to temperatures of up to 250 °C are shown in Table 1.

The Maya Yellow sample was prepared from palygorskite and isatin. Yet, washing with acetone after the heating step led to a rather off-white or pale ochre solid. To obtain further new colorful pigments based on isatin, palygorskite was treated with a mixture of indigo and isatin (1:5 and 2:5, w/w, Maya Green 15 and 25) and heated to form green pigments (Table 1). Maya Green 25 with a higher amount of indigo showed a more blueish green color than Maya Green 15.

XRD measurements were carried out with the new pigments for phase analysis (Fig. 3). As can be seen, the diffractogramms of Sepi-Br2, Sepi-Cl2 and Sepi-Blue matched the two reference diffractograms found for sepiolite. All peaks were identified and there were no differences between the three samples, i.e. they had the same crystal structure. The samples Maya-Br2, Maya-Cl2, Maya-F2 and Maya-Yellow all exhibited three different phases: palygorskite-O, calcite and quartz. Again, there were no discernible differences between the four samples, although the palygorskite-O phase seemed to be less pronounced for Maya-Br2. However, since no quantitative Riedveld analysis was performed, this couldn't be confirmed.

Solid state UV-VIS spectroscopy was carried out for the new palygorskite- and sepiolite-based pigments (Fig. 4). The pigments showed only moderate reflectance in the UV region. The blue pigments (Blue, F2, Cl2, Br2) have a local reflectance maximum between 400 and 450 nm, which matches with published data of Maya Blue and the analogous sepiolite-based pigments of indigo and 6,6′-dibromoindigo [29,33].

In contrast, the olive green pigments (MeO4 and OMeO2) exhibited a minimum in this region, followed by a local maximum between 500 and 550 nm. Reflectance increases from 670 nm towards the IR region where it reaches approx. 70–80 %. Reflectance of the green samples (MeO4, OMeO2, Green 15/25) was lower when compared with the blue samples. The spectrum of Maya Yellow differed from the spectra of the other pigments and showed similarities with spectra of samples from the Maya site Mayapán [12]. All spectra displayed a peak at 623 nm, which can be neglected since the applied detector generates a reproducible error at this wavelength.

The crude pigments obtained upon heating to 150 °C for 22 h were purified by washing with hot organic solvent (acetone) for several hours in order to remove unreacted dye. The colors of the purified/washed pigments and the stability of the pure pigments up to a temperature of 270 °C were investigated (Table 2). The pigments did not change their color upon heating to 230 °C, 250 °C, and 270 °C for 15 min. Thus, the pigments possess temperature stabilities comparable with published stability data of Maya Blue.

Calorimetric data were obtained during the heating process starting from freshly prepared mixtures of the corresponding dye with palygorskite or sepiolite (Table 3). While heating up the samples two different transitions appeared for each sample. The first transition was correlated with the evaporation of water. Palygorskite and sepiolite differed from each other regarding the amount of water in the sample. For palygorskite, the specific enthalpy of evaporation was ~25 J/g to 30 J/g, the sepiolite samples contained twice as much water and showed ~50 J/g at the first transition. Both samples showed a second transition at higher temperatures. For palygorskite this transition started at ~180 °C and had an enthalpy of ~20 J/g. For sepiolite, this effect was
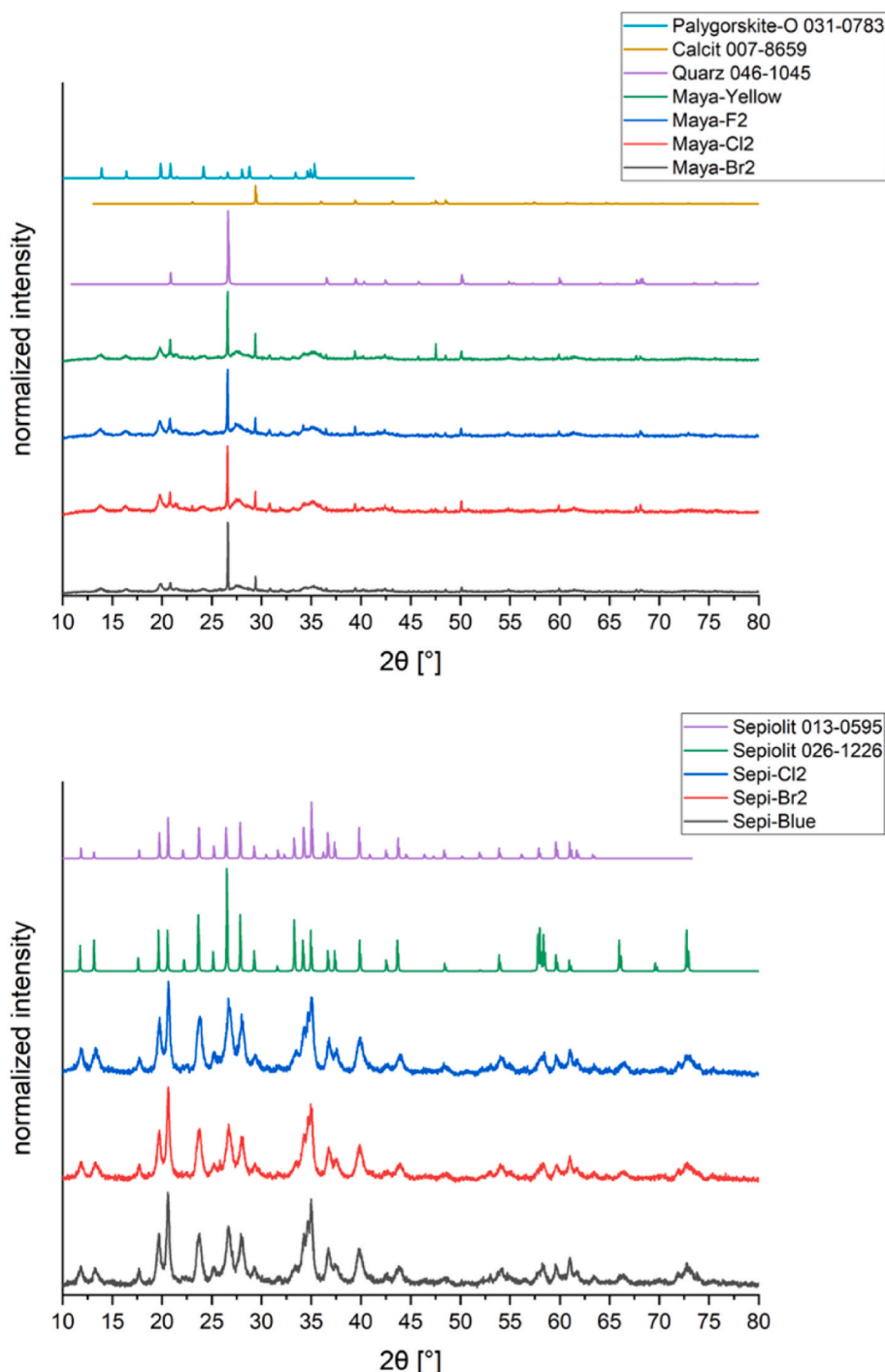
Fig. 3. Diffractograms of pigment powders based on palygorskite (top) and sepiolite (bottom).

not reproducible and fluctuated or did not appear at all. One reason for this effect could be the exothermal decomposition of the sample at ~300 °C. Comparing the washed samples and the unwashed samples, no significant differences of the DSC signal were visible. In contrast, the optical differences were significant because of colored spots on the sample while heating.

The temperature stability was not influenced significantly by the sort of pigments used either. Without any change of color, the decomposition started nearly at the same temperatures. The results of color change were also reproducible for the different types of samples. The raw materials themselves also changed their color slightly while heating because of evaporating water. However, this change was small and,

thus, it was ignored for the evaluation of the samples.

Previous studies evaluated the relevance of indigo decomposition during Maya Blue preparation at higher temperatures. Since the decomposition point of indigo does not differ between free and clay-bound forms, it is unlikely that decomposition processes have an influence on the colors of the resulting pigments at reaction temperatures of 150 °C. The color changes between indigo dye and Maya Blue pigment were rather associated with crucial edge silanol-indigo interactions upon release of zeolite water [34].

Raman spectra of the pigments were recorded from 267 to 2005 cm^{-1} and exhibited distinct features of the applied indigo molecules (Fig. 5 and Fig. S1). In particular, strong signals of stretching C=C of the
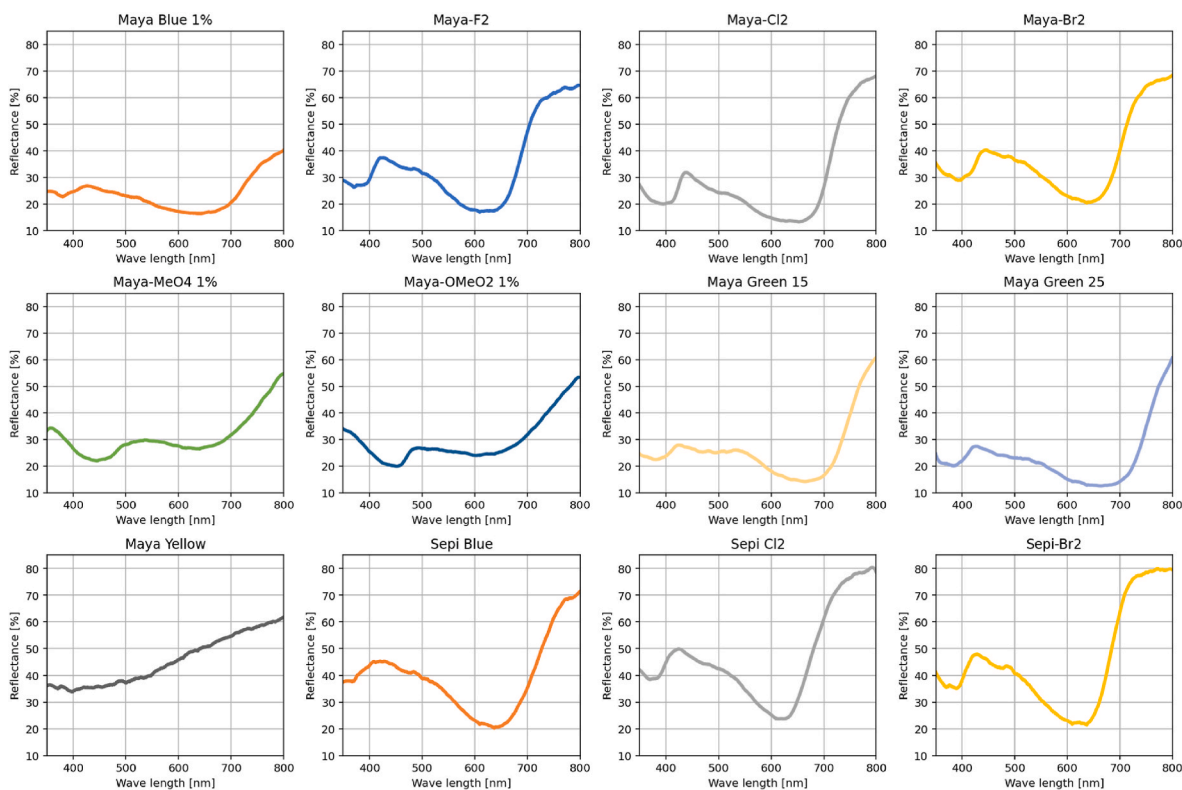
Fig. 4. UV-VIS spectra of the indicated pigment powders.

Table 3
Onset temperatures and enthalpies for the two transition temperatures of the samples.

Compd.	T_{O1} [°C]	H_1 [J/g]	T_{O2} [°C]	H_2 [J/g]
Palygorskite	71.0	−29.15	173.0	−19.91
Sepiolite	50.8	−52.46	265.5	−26.09
Maya Blue (1 %)	63.8	−25.85	180.3	−22.6
Maya Thio	71.4	−25.74	–	–
Maya Yellow	73.2	−25.52	193.7	−22.93
Maya-Cl2 (1 %)	70.4	−25.10	171.8	−21.38
Maya-Br2	72.4	−25.36	179.5	−23.26
Maya-F2	68.0	−25.76	173.6	−24.98
Maya-MeO4	78.8	−26.11	186.3	−22.73
Maya-OMeO2	68.3	−25.93	162.1	−24.67
Maya Green 15	76.0	−26.00	185.3	−22.50
Maya Green 25	76.9	−27.50	174.9	−23.20
Sepi Blue	56.2	−25.29	–	–
Sepi-Cl2	56.2	−51.23	35.0	−23.74

T_{O1}: onset temperature 1; H_1: enthalpy 1; T_{O2}: onset temperature 2; H_2: enthalpy 2.

indigo molecules were observed (1550–1590 cm^{-1}) in the spectra of the pigment samples, which are in line with published Raman spectroscopic data of indigo and its derivatives [21,35,36]. A closer look at this signal in the spectra of the palygorskite-based pigments revealed some differences in terms of location and intensity between the pigments depending on the indigo derivative (Fig. 5A). Among the sepiolite-based pigments, Sepi-Cl2 showed higher signal intensities than Sepi-Br2 (Fig. 5B).

3.2. Thermal gravimetric analyses and differential scanning calorimetry

Thermal gravimetric analysis (TGA) measurements were carried out in order to investigate the thermal stability of the pigments (Figs. 6–9). Maya-Cl2 showed relatively small mass loss at higher temperatures (>600 °C) when compared with the other palygorskite-based pigments and pure palygorskite (Fig. 6). In contrast to that, Maya Yellow exhibited

distinctly higher mass losses than palygorskite and the other palygorskite-based pigments upon heating (already at 200 °C). The differences are not very distinct in the sepiolite series (Fig. 7). Only at temperatures above 800 °C, the Sepi-Cl2 and Sepi-Br2 pigments showed higher mass losses when compared with sepiolite and Sepi Blue. DSC measurements were carried out in order to determine the heat flow caused by the pigments upon heating. Maya-Cl2 showed a relatively low heat flow at temperatures above 700 °C (Fig. 8). Interestingly, Maya-MeO4 exhibited a relatively high heat flow over the temperature range from 200 °C to 1000 °C. High heat flow values were also observed for Sepi Blue above temperatures of 400 °C when compared with the other sepiolite-based pigments and pure sepiolite. Sepi-Cl2 displayed lower heat flow values than sepiolite and the sepiolite-based pigments (Fig. 9). All pigment samples were charred and black after the tests and heating to 1000 °C due to decomposition of the bound indigo molecules.

3.3. Scanning electron microscopy

Scanning electron microscopy (SEM) was applied for the determination of the nanostructure of palygorskite and selected palygorskite-based pigments (Maya Blue, Maya-Cl2, and Maya-Br2). The obtained SEM images showed the fibrous structure of palygoskite, which was retained in the pigments Maya Blue, Maya-Cl2 and Maya-Br2 (Fig. 10). However, this method is limited to clay crystal aggregates and voltammetry might be more suitable for in-depth studies of Maya Blue pigment microparticles [10,37].

3.4. Combustion of cellulose acetate mixtures with Maya Blue or Maya-Cl2

Aside their function as a dye, pigments can also possess additional properties improving the utilities of the dyed material. Hence, Maya Blue and Maya-Cl2 pigments were selected for studies concerning their suitability as flame retardants in polymer mixtures. Cellulose acetate (CA) was chosen as polymer for these combustion tests and mixtures of
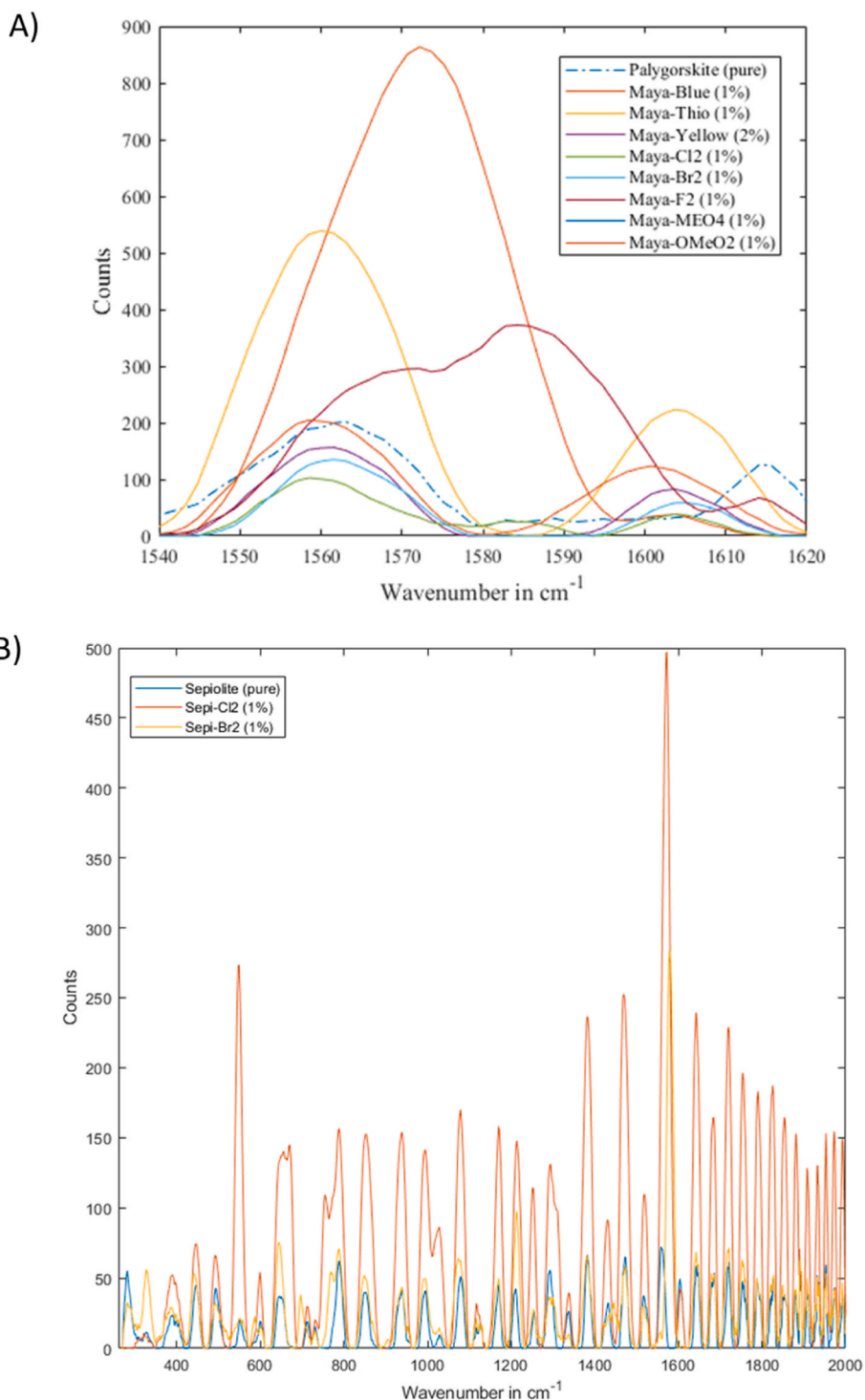
Fig. 5. Raman spectra of the indicated pigments based on palygorskite (A, enlarged segment between 1540 and 1620 cm^{-1}) and sepiolite (B, complete spectra from 267 to 2005 cm^{-1}).

CA with palygorskite or with the mentioned pigments were prepared and analyzed. The time-dependent heat release rate (HRR) curves of pure CA and of the mixtures of CA with palygorskite (4.4 %, w/w) or pigments Maya Blue and Maya-Cl2 (each 4.4 %, w/w) are shown below (Fig. 11). Already the addition of palygorskite can reduce the peak heat release rate (PHHR) significantly. The modified Maya pigments, which are composites of palygorskite with indigo or 6,6′-dichloroindigo, did not deteriorate the heat release rate reducing activity of palygorskite. Quite the opposite, both mixtures with Maya-Cl2 pigments and the

mixture with MB2% could slightly improve the HRR effect of palygorskite.

The combustion data of CA and its mixtures with palygorskite or with the pigments Maya Blue and Maya-Cl2 are given in Table 4. The CA mixtures with pigments showed distinctly stronger PHRR reduction (reduction by 22–23 %) when compared with pure CA. Although the observed flame retardancy is mainly attributed to the palygorskite silicate material, the pigment mixtures also performed slightly better than palygorskite concerning PHRR reduction of the CA material indicating a
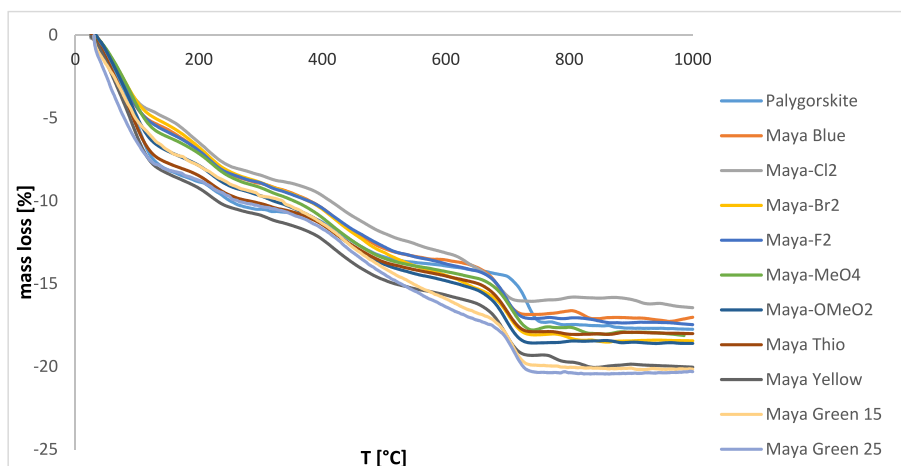
Fig. 6. Temperature-dependent thermal gravimetric (TG) analysis measurement of the pure pigments based on palygorskite.
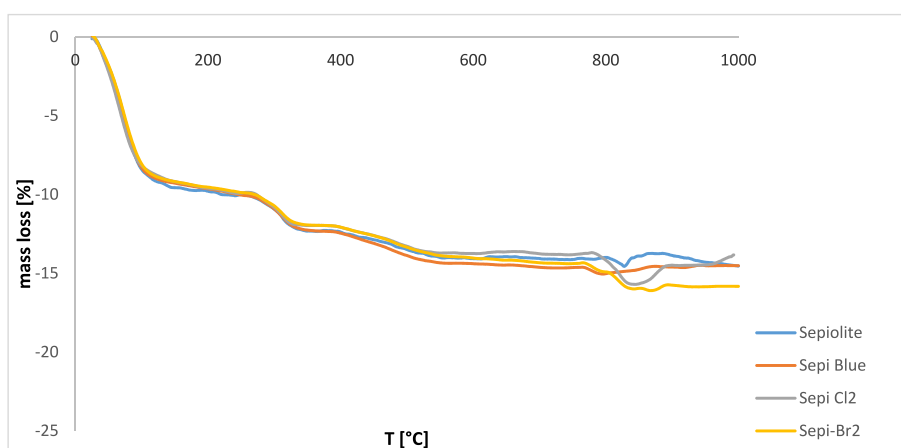
Fig. 7. Temperature-dependent thermal gravimetric (TG) analysis measurement of the pure pigments based on sepiolite.
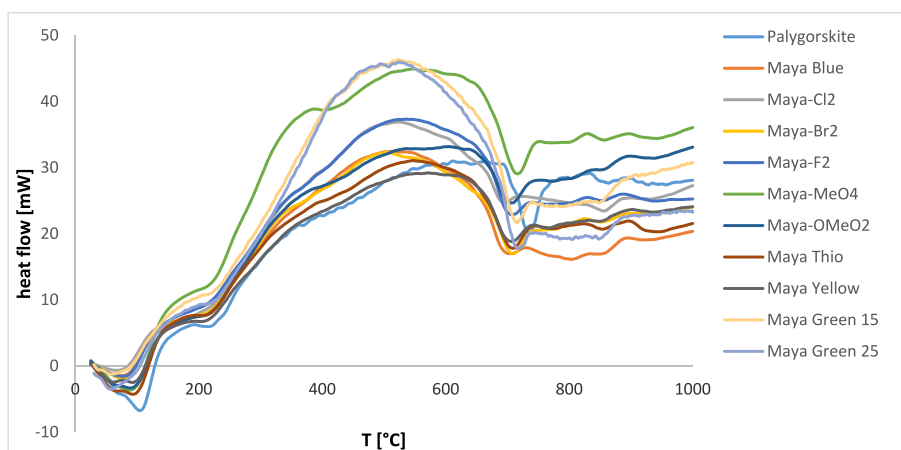
Fig. 8. Differential scanning calorimetry (DSC) measurement of the pure pigments based on palygorskite ("Maya" series).

small influence of the heteroaromatic indigo molecules which might be enhanced by using higher indigo contents in the pigments. In addition, the observed PHRR values of the pigments in CA were in the range of previously investigated synthetic and natural flame retardants for CA such as the DOPO-melamine salt MDOP and salmon DNA [38,39]. Representative photographs of the charred material upon combustion can be found in the supplementary material (Figs. S2–S4).

The total heat release (THR) and total smoke release (TSR) was slightly higher for the pigment mixtures when compared with the palygorskite mixture and with pure CA. The time to ignition (t_{ig}) of all pigment mixtures was in the range of pure CA but distinctly shorter than that of palygorskite. The high water content of commercially available palygorskite might be an explanation for this discrepancy.

Values of CO_x formation and O_2 consumption during combustion of
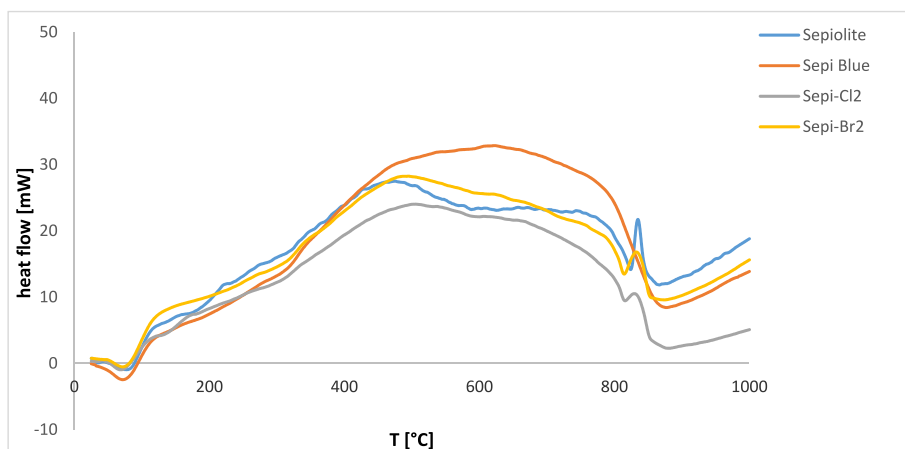
Fig. 9. Differential scanning calorimetry (DSC) measurement of the pure pigments based on sepiolite ("Sepi" series).

Fig. 10. SEM images of pigments (Maya Blue, Maya-Cl2, and Maya-Br2) and of palygorskite as reference material.

Fig. 11. Time-dependent heat release rate (HRR) curves of pure CA and of CA mixtures (4.4 %, w/w) with palygorskite, Maya Blue (MB, 1 % or 2 % indigo), or Maya-Cl2 (MCl2, 1 % or 2 % 6,6′-dichloroindigo).

Table 4
Combustion data of pure CA and of its mixtures (4.4 %, w/w) at the indicated concentrations.
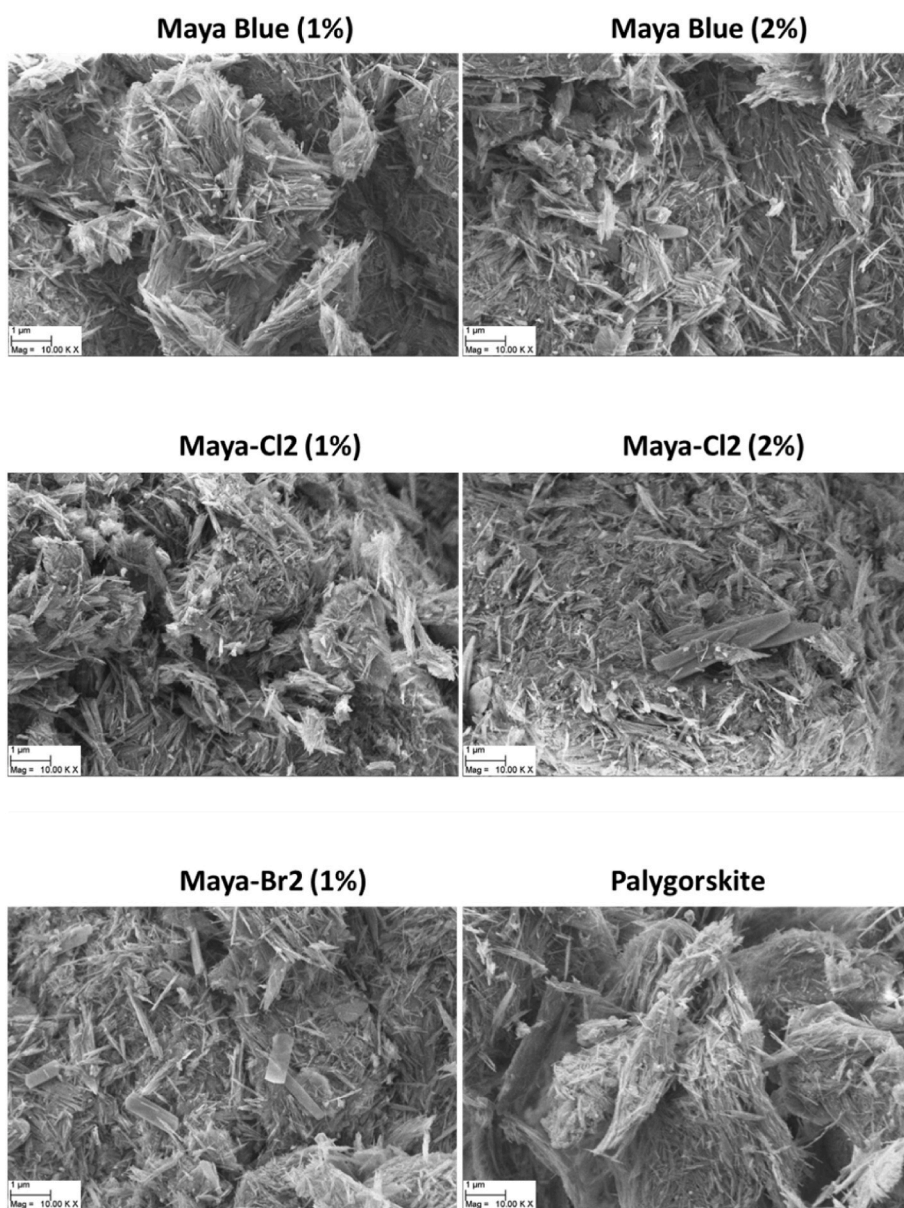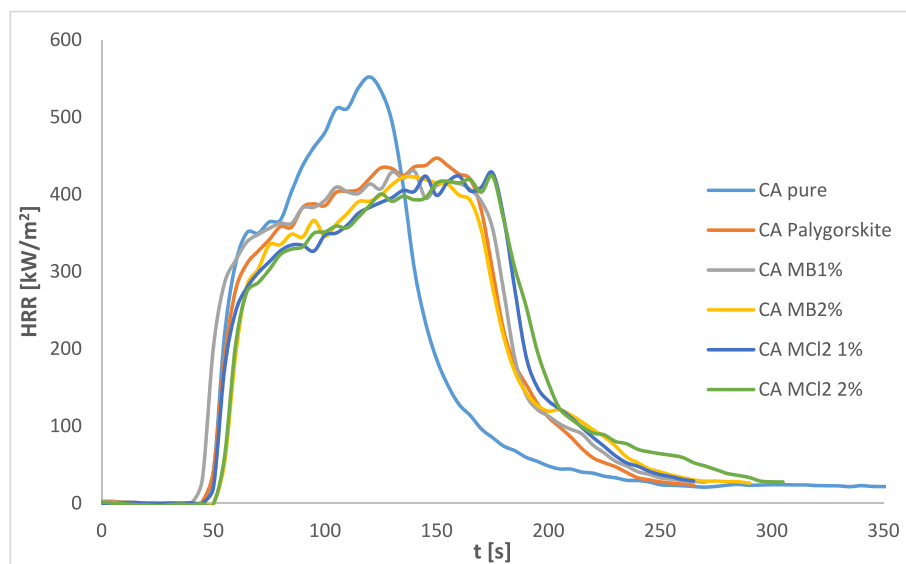
Compd.	PHRR (kW/m^2)	PHRR red. (%)	THR (MJ/m^2)	TSR (m^2/m^2)	t_{ig} (s)
CA	552	-	50.3	84.8	53
CA-Palygorskite	447	19.0	48.3	101.5	78
CA-Maya Blue (1 %)	430	22.1	57.1	122.8	49
CA-Maya Blue (2 %)	422	23.6	52.6	113.9	57
CA-Maya-Cl2 (1 %)	428	22.5	54.4	120.7	53
CA-Maya-Cl2 (2 %)	424	23.2	56.6	121.4	56

PHRR: peak of heat release rate; PHRR red.: PHRR reduction when compared with pure CA; THR: total heat release; TSR: total smoke release; t_{ig}: time to ignition.

CA and the pigment mixtures are provided in Table 5. The palygorskite and pigment mixtures showed a distinctly lower carbon monoxide (CO) release when compared with pure CA. The mechanism how palygorskite reduces CO release during CA combustion remains to be elucidated. However, polymer blends with minerals such as hydromagnesite and huntite were also able to suppress CO levels, while the zeolite-modified palygorskite material ZIF-67@ATP delayed CO formation at early stages of combustion [40,41]. The formation of carbon dioxide (CO_2) by the pigment mixtures did not differ much from the CO_2 formation by pure CA upon combustion. O_2 consumption was slightly increased in the CA mixtures with Maya pigments when compared with pure CA.

Table 5
CO_X formation and O_2-consumption during combustion of pure CA and of its mixtures (4.4 %, w/w) at the indicated concentrations.

Compd.	CO (kg/kg)	CO_2 (kg/kg)	O_2 consumption (g)
CA	0.060	1.47	34.1
CA-Palygorskite	0.019	1.56	32.6
CA-Maya Blue (1 %)	0.016	1.48	38.2
CA-Maya Blue (2 %)	0.017	1.44	35.4
CA-Maya-Cl2 (1 %)	0.014	1.43	36.6
CA-Maya-Cl2 (2 %)	0.018	1.44	38.1

CO: median CO formation; CO_2: median CO_2 formation.

4. Conclusions

A series of new pigments related to Maya Blue were prepared and investigated for their thermal properties. The results were compared with the properties of known Maya Blue pigments including the thio-indigo- and isatin-based derivatives. The investigation of DSC in combination with an optical camera gave valuable information about the thermal stability of various pigments. The pigments Maya Blue and Maya-Cl2 were selected for further testing as flame retardants in polymer mixtures with cellulose acetate and led to significant heat release rate reduction and reduced formation of toxic CO. The studied "Maya" pigments don't contain environmentally problematic heavy metals such as Cu and Co (in contrast to other common blue and/or green pigments), and thus can be useful for manifold applications.

CRediT authorship contribution statement

Michael Gerlach: Writing – review & editing, Writing – original draft, Methodology, Investigation, Formal analysis, Conceptualization. **Justus Koedel:** Writing – review & editing, Writing – original draft, Methodology, Investigation, Formal analysis, Conceptualization. **Sebastian Seibt:** Writing – review & editing, Writing – original draft, Methodology, Investigation, Formal analysis, Conceptualization. **Benjamin Baumgärtner:** Data curation, Formal analysis, Investigation. **Christoph Callsen:** Writing – original draft, Methodology, Investigation, Formal analysis. **Gundula Voss:** Writing – review & editing, Methodology, Investigation, Formal analysis, Conceptualization. **Florian Puchtler:** Writing – review & editing, Methodology, Investigation, Formal analysis. **Andy Weidinger:** Writing – review & editing, Supervision, Resources, Project administration, Conceptualization. **Georg Puchas:** Writing – review & editing, Methodology, Investigation, Formal analysis. **Daniel Leykam:** Writing – review & editing, Methodology, Investigation, Formal analysis. **Volker Altstaedt:** Writing – review & editing, Supervision, Resources, Project administration, Funding acquisition, Conceptualization. **Rainer Schobert:** Writing – review & editing, Supervision, Resources, Project administration, Funding acquisition, Conceptualization. **Holger Ruckdäschel:** Writing – review & editing, Supervision, Resources, Project administration, Funding acquisition, Conceptualization. **Bernhard Biersack:** Writing – review & editing, Writing – original draft, Supervision, Project administration, Methodology, Investigation, Formal analysis, Conceptualization.

Declaration of competing interest

The authors declare that they have no known competing financial interests or personal relationships that could have appeared to influence the work reported in this paper.

Acknowledgements

Appendix A. Supplementary data

Supplementary data to this article can be found online at https://doi.org/10.1016/j.dyepig.2024.112530.

Data availability

Data will be made available on request.

References

[1] Berke H. The invention of blue and purple pigments in ancient times. Chem Soc Rev 2007;36:15–30.

[2] Berke H. Chemistry in ancient times: the development of blue and purple pigments. Angew Chem Int Ed 2002;41:2483–7.

[3] Sánchez-del Río M, Doménech A, Doménech-Carbó MT, Vázquez de Agredos Pascual ML, Suárez M, García-Romero E. The Maya blue pigment. In: Galan E, Singer A, editors. Developments in Clay Science, Vol. 3. Developments in palygorskite-sepiolite research – a new outlook on these nanomaterials. Elsevier B. V.; 2011. p. 453–81.

[4] Van Olphen H. Maya Blue: a clay-organic pigment? Science 1966;154:645–6.

[5] Reinen D, Köhl P, Müller C. The nature of the colour centres in 'Maya Blue' – the incorporation of organic pigment molecules into the palygorskite lattice. Z Anorg Allg Chem 2004;630:97–103.

[6] Li L, Zhuang G, Li M, Yuan P, Deng L, Guo H. Influence of indigo-hydroxyl interactions on the properties of sepiolite-based Maya blue pigment. Dyes Pigments 2022;200:110138.

[7] Bernardino ND, Constantino VRL, de Faria DLA. Probing the indigo molecule in Maya Blue simulants with resonance Raman spectroscopy. J Phys Chem C 2018; 122:11505–15.

[8] Doménech-Carbó A, Holmwood S, di Turo F, Montoya N, Valle-Algarra FM, Edwards HGM, Doménech-Carbó MT. Composition and color of Maya Blue: reexamination of literature data based on the dehydroindigo model. J Phys Chem C 2019;123:770–82.

[9] Doménech-Carbó A, Costero AM, Gil S, Montoya N, López-Carrasco A, Sáez JA, Arroyo P, Doménech-Carbó MT. Isomerization and redox tuning: reorganizing the Maya Blue puzzle from synthetic, spectral, and electrochemical issues. J Phys Chem C 2021;125:26188–200.

[10] Doménech A, Doménech-Carbó MT, de Agredos Pascual MLV. Dehydroindigo: a new piece into the Maya Blue puzzle from the voltammetry of microparticles approach. J Phys Chem B 2006;110:6027–39.

[11] Sánchez del Río M, Martinetto P, Reyes-Valerio C, Dooryhée E, Suárez M. Synthesis and acid-resistance of Maya blue pigment. Archaeometry 2006;48:115–30.

[12] Doménech A, Doménech-Carbó MT, Vázquez de Agredos-Pascual ML. From Maya Blue to "Maya Yellow": a connection between ancient nanostructured materials from the voltammetry of microparticles. Angew Chem Int Ed 2011;50:5741–4.

[13] Zhou W, Liu H, Xu T, Jin Y, Ding S, Chen J. Insertion of isatin molecules into the nanostructure of palygorskite. RSC Adv 2014;4:51978–83.

[14] Rondao R, Seixas de Melo JS. Thio-Mayan-like compounds: excited state characterization of indigo sulfur derivatives in solution and incorporated in palygorskite and sepiolite clays. J Phys Chem C 2013;117:603–14.

[15] Fan L, Zhang Y, Zhang J, Wang A. Facile preparation of stable palygorskite/cationic red X-GRL@SiO₂ "Maya Red" pigments. RSC Adv 2014;4:63485–93.

[16] Zhang Y, Zhang J, Wang A. Facile preparation of stable palygorskite/methyl violet@SiO₂ "Maya Violet" pigment. J Colloid Interface Sci 2015;457:254–63.

[17] Chianelli RR, Niewold LA, Williams G. Organic/Inorganic complexes as color compositions. WO 2008/097837 A2.

[18] Roy M. Dyes in ancient and medieval India. Indian J Hist Sci 1978;13:83–112.

[19] Fernelius WC, Renfrew EE. Indigo. J Chem Educ 1983;60:633–4.

[20] Baeyer A, Drewsen V. Darstellung von Indigblau aus Orthonitrobenzaldehyd. Ber Dtsch Chem Ges 1882;15:2856–64.

[21] Cooksey CJ. Tyrian purple: 6,6'-dibromoindigo and related compounds. Molecules 2001;6:736–69.

[22] Voß G, Gerlach H. Regioselektiver Brom/Lithium-Austausch bei 2,5-Dibrom-1-nitrobenzol. – Eine einfache Synthese von 4-Brom-2-nitrobenzaldehyd und 6,6'-Dibromindigo. Chem Ber 1989;122:1199–291.

[23] Tanoue Y, Sakata K, Hashimoto M, Hamada M, Kai N, Nagai T. A facile synthesis of 6,6'- and 5,5'-dihalogenoindigos. Dyes Pigments 2004;62:101–5.

[24] Klimovich IV, Leshanskaya LI, Troyanov SI, Anokhin DV, Novikov DV, Piryazev AA, Ivanov DA, Dremova NN, Troshin PA. Design of indigo derivatives as environment-friendly organic semiconductors for sustainable organic electronics. J Mater Chem C 2014;2:7621–31.

[25] Seixas de Melo JS, Rondao R, Burrows HD, Melo MJ, Navaratnam S, Edge R, Voss G. Spectral and photophysical studies of substituted indigo derivatives in their keto forms. ChemPhysChem 2006;7:2303–11.

[26] Voss G, Gradzielski M, Heinze J, Reinke H, Unverzagt C. Highly soluble and green indigo dyes: 4,4',7,7'-tetraalkoxy-5,5'-diaminoindigotins. Helv Chim Acta 2003;86: 1982–2004.

[27] Glowacki ED, Voss G, Leonat L, Irimia-Vladu M, Bauer S, Sariciftci NS. Indigo and Tyrian purple – from ancient natural dyes to modern organic semiconductors. Isr J Chem 2012;52:540–51.

[28] Irimia-Vladu M, Glowacki ED, Voss G, Bauer S, Sariciftci NS. Green and biodegradable electronics. Mater Today 2012;15:340–6.

[29] Winum J-Y, Bernaud L, Filhol J-S. The hunt for Maya Purple: revisiting ancient pigments syntheses and properties. J Chem Educ 2021;98:1389–96.

[30] Kiliaris P, Papaspyrides CD. Polymer/layered silicate (clay) nanocomposites: an overview of flame retardancy. Prog Polym Sci 2010;35:902–5.

[31] García-Romero E, Suárez M. Sepiolite-palygorskite: textural study and genetic considerations. Appl Clay Sci 2013;86:129–44.

[32] Almeida R, Ferraz E, Santarén J, Gamelas JAF. Comparison of surface properties of sepiolite and palygorskite: surface energy and nanoroughness. Nanomaterials 2021;11:1579.

[33] Grazia C, Buti D, Amat A, Rosi F, Romani A, Domenici D, Sgamellotti A, Miliani C. Shades of blue: non-invasive spectroscopic investigations of Maya blue pigments. From laboratory mock-ups to Mesoamerican codices. Herit Sci 2020;8:1.

[34] Hubbard B, Kuang W, Moser A, Facey GA, Detellier C. Structural study of Maya Blue: textural, thermal and solid-state multinuclear magnetic resonance characterization of the palygorskite-indigo and sepiolite-indigo adducts. Clay Clay Miner 2003;51:318–26.

[35] Baran A, Fiedler A, Schulz H, Baranska M. In situ Raman and IR spectroscopic analysis of indigo dye. Anal Methods 2010;2:1372–6.

[36] Bayerová T. Buddhist wall paintings at Nako Monastery, North India: changing of the technology throughout centuries. Stud Conserv 2018;63:171–88.

[37] Doménech A, Doménech-Carbó MT, de Agredos Pascual MLV. Chemometric study of Maya Blue from the voltammetry of microparticles approach. Anal Chem 2007; 79:2812–21.

[38] Koedel J, Callsen C, Weise M, Puchtler F, Weidinger A, Altstaedt V, Schobert R, Biersack B. Investigation of melamine and DOPO-derived flame retardants for the bioplastic cellulose acetate. Polym Test 2020;90:106702.

[39] Koedel J, Seibt S, Callsen C, Puchtler F, Weise M, Weidinger A, Altstaedt V, Ruckdäschel H, Schobert R, Biersack B. DNA as a natural flame retardant for cellulose acetate polymer mixtures. ChemistrySelect 2021;6:3605–9.

[40] Hollingbery LA, Hull TR. The fire retardant behaviour of huntite and hydromagnesite – a review. Polym Degrad Stabil 2010;95:2213–25.

[41] Ma D-X, Yang Y, Yin G-Z, Vázquez-López A, Jiang Y, Wang N, Wang D-Y. ZIF-67 in situ grown on attapulgite: a flame retardant synergist for ethylene vinyl acetate/magnesium hydroxide composites. Polymers 2022;14:4408.